THE ASTROPHYSICAL JOURNAL, 404:L25–L27, 1993 February 10

ASTROPHYSICAL GASDYNAMICS CONFRONTS REALITY: THE SHAPING OF PLANETARY NEBULAE

ADAM FRANK[1]
Astronomy Department, University of Washington
BRUCE BALICK[2]
Astronomy Department, University of Washington, and Sterrewacht Leiden, Leiden University
AND
VINCENT ICKE[2] AND GARRELT MELLEMA[3]
Sterrewacht Leiden, Leiden University
Received 1992 September 9; accepted 1992 November 25

ABSTRACT

We present two-dimensional numerical simulations, which use techniques of radiation gasdynamics to simulate the structures of planetary nebulae (PNs). Our model incorporates realistic volume emissivities in order to fully account for the conversion of mechanical and thermal energy into radiation. The model also produces detailed predictions of observables such as projected structure (e.g., Hα and [N II] images) and kinematic patterns. Virtually the full range of PN morphologies are easily reproduced, as are the basic kinematics, ionization structures, and temperatures.

Subject headings: hydrodynamics — planetary nebulae: general — stars: kinematics — stars: mass loss

1. INTRODUCTION

Planetary nebulae (PNs) have shapes ranging from round through elliptical to bipolar. Balick (1987, hereafter B87) suggested that the morphologies and the kinematics might be explained within one framework; a fast stellar wind that interacts hydrodynamically with a concentric, dense toroid ejected earlier. Outflow patterns, which become preferentially aligned to the toroid's symmetry axis, produce prolate or, eventually, bipolar PNs. A quantitative understanding of the shaping process can provide insight into the origin and evolution of the shapes of PNs while, at the same time, helping to sharpen the methodologies of astrophysical techniques in preparation for tackling more complex or elusive classes of problems such as AGNs and H-H objects (Icke, Balick, & Frank 1992a, hereafter IBF92).

The success of two-dimensional numerical simulations in accounting for the shapes and kinematics of PNs has been growing steadily (e.g., Kahn & West 1985; Balick, Preston, & Icke 1987, hereafter BPI87; Soker 1989, 1990; Icke, Preston, & Balick 1989, hereafter IPB89; Icke 1991; Mellema, Eulderink, & Icke 1991; hereafter MEI91; IBF92). However, none of these simulations have properly accounted for energy loss through radiation. The possible importance of radiative energy loss to the growth of the nebula has been repeatedly stressed and, to an extent, explored in one dimension (Kwok & Volk 1985; Kahn & Breitschwerdt 1990).

Such radiation gasdynamic calculations are the crucial link in the connection between models and observations. Volume emissivities of all bright emission lines, the radio and optical continuum, and even soft X-rays are intrinsic to the computations in two dimensions. The results can be spun around their symmetry axis into three dimensions, tilted, and projected onto the sky in order to produce predictions of the density distribution, ionization structure, kinematics, etc., which are readily comparable to observations. Here we summarize numerical experiments in which radiation processes have been incorporated, and we demonstrate their success. A more complete description of the results is being prepared for future publication.

2. METHODOLOGY AND RESULTS

A comprehensive description of the model and the numerical techniques is impossible here; see IBF92, Frank (1992), Frank & Mellema (1993), and Frank (1993) for various details. Energy loss via radiation is treated as one of several cooling terms in the energy density equation. The radiation subroutine invokes calculations of the time- and space-dependent transfer of stellar UV photons, and computes (among other parameters) the resulting states and time derivatives of ionization rates, recombination rates, heating, and many types of radiative cooling rates (including thermal bremsstrahlung and all significant thermally excited forbidden lines[4]). Ionization equilibrium was assumed for elements heavier than He. We have not included heating and cooling from dust grains in the energy budget of the models. While dust is important in young PNs (Zhang & Kwok 1991), limited computational resources have forced us to neglect its influence in the model. We expect, however, that including dust will only affect the inner regions of the nebulae and will produce more acceleration and more cooling during the early stages of model evolution.

Initial and boundary conditions are described in IBF92 (see

[1] Postal address: Department of Astronomy, University of Minnesota, 116 Church St. S.E., Minneapolis, MN 55455.
[2] Postal address: Astronomy Department FM-20, University of Washington, Seattle, WA 98195.
[3] Postal address: Sterrewacht Leiden, Postbus 9513, 2300RA Leiden, The Netherlands.
[4] At temperatures below 10^5 K the radiative energy losses and volume emissivities of thermally excited forbidden lines of N^+, O^+, O^{++}, Ne^{++}, C^{3+}, and N^{4+} are computed by approximating the results of full 5-level computations with a more computationally efficient power series fit as functions of electron temperature and density (Balick et al. 1993). At higher temperatures the coronal cooling rates of Dalgarno & McCray (1972) are used.

their eqs. [8] and [9]). To summarize: $1 - \alpha$ is the pole-to-equator density contrast; β governs the shape of the inner part of the disk; smaller (larger) values of β generally yield elliptical (bipolar) PNs (see MEI91, Figs. 1, 2). Moderate values of $\alpha = 0.7$ and $\beta = 3$ are used for the present illustrative models. A (spherically symmetric) fast wind mass-loss rate of $\dot{M}_{\rm fw} = 1.3 \times 10^{-7}\ M_\odot\ {\rm yr}^{-1}$, outflow velocity $v_{\rm fw}$ of 10^3 km s^{-1}, photospheric and minimum wind temperature of 50,000 K, and stellar radius of 0.05 $R_\odot$ are also assumed. The stellar parameters are turned on instantaneously at time = 0 which causes an artificially fast development time scale at first. The grid consists of 100 × 100 cells each with radial size = 2×10^{15} cm. Models were run on the Cray Y-MP of the San Diego Supercomputer Centre.

It is impossible to present the full set of time-dependent model results. A representative sample appears in Figure 1 (Plate L2): the distribution of density, temperature, radial velocity and tangential velocity are displayed logarithmically versus position after 900 years of evolution. The interaction between the fast wind and the toroid produces the classic two-wind "interacting stellar winds" (ISW) shock flow pattern (e.g., Dyson & Williams 1980), the main features of which are described by IBF92. The interior is a high-temperature (10^7 K), low-density (1 cm^{-3}) optically invisible bubble whose relatively high pressure drives a shock into the cooler gas ahead. Ellipticity or bipolarity forms quickly once the dimensions of the expanding bubble and toroid along the symmetry axis become comparable. At 900 yr the density of the swept-up gas outside the bubble varies from 5000 (equator) to 800 cm^{-3} (pole). Such densities are characteristic of the bright rims of PNs that surround central "cavities" of NGC 3242 and 7662 (e.g., Balick et al. 1993).

A comparison of the radial and transverse velocities in Figure 1 shows (1) a sharp drop in the radial velocity at the inner, or reverse, shock inside the bubble, (2) higher radial velocities at higher latitudes within the bubble (without which a bipolar will not form), (3) some stagnation regions midway between the inner shock and the bubble's leading edge (contact discontinuity), (4) a slight corrugation instability along the inner shock with size scales of a few cells (these could be artifacts of the grid used), and (5) rippling of the flow as it enters the bubble interior.

It is of interest to compare the present computational models with radiationless, that is, adiabatic, models with much the same initial conditions (IBF92; MEI91). The adiabatic models cannot cool as efficiently, especially in the swept-up gas where radiative cooling is highly efficient. In the bubble we find that the temperatures are ≈2–3 times less than for adiabatic models. In the swept-up gas and beyond we find $T \approx 10^4$ K, as observed, whereas the temperature is ≈10 times higher without radiative cooling. Since cooling rates tend to scale as (density)^2, and heating scales more slowly, the small thermal gradient from equator to pole is caused by the decreasing densities.

3. "NUMERICAL OBSERVATIONS"

Our attention now turns to the observables generated by the simulations and their comparison to actual data. Again, only a brief synopsis and some illustrative results can be given here. To begin, note that the expansion velocities of the optically bright swept-up gas are 125 km s^{-1} along the pole and 30 km s^{-1} along the equator, in excellent agreement with observations of several bipolars by IPB89. Further discussion of nebular kinematics will be deferred to future papers.

Figure 2 (Plate L3) shows the results of the model of Figure 1 reproduced as tilted and sky-projected two-dimensional images in the light of Hα. Intensities are displayed logarithmically in order to show the full range of structures. Also shown are images of likely nebular counterparts from B87.

The success at matching PN morphologies is striking, even for this small subset of the full set of results. At lower inclination angles some of the main features are "barrels" formed by the swept-up gas at low latitudes and short, stubby bipolar lobes along the symmetry axis at higher latitudes. NGC 40, 2610, 7048, 7139, 7354, IC 289, Abell 82, and M2-51 are PNs which share most or all of these features. At $i = 45°$ the nebula appears as an "8" with a surrounding elliptical shell, much as the Owl Nebula (NGC 3587), the Helix Nebula (NGC 7293), and perhaps NGC 1514.

At still higher inclinations the nebulae appear increasingly round. Images alone do not distinguish between intrinsically round and highly inclined elliptical or bipolar PNs. However, kinematic studies easily resolve the ambiguities. An interesting example is the Eskimo Nebula (NGC 2392) which has been studied in detail by O'Dell, Weiner, & Chu (1990) and BPI87. Both groups suggest that this round nebula is a very highly inclined bipolar PN. Another example could be the Ring Nebula (NGC 6720), although Balick et al. (1992) argue to the contrary on the basis of morphological evidence beyond the scope of this paper. PNs such as NGC 3242, 6894, 7662, IC 1454, 3568, Abell 30, and He 1-4 appear to be intrinsically round or mildly elliptical.

Models with different sets of toroidal parameters or at earlier or later evolutionary phases yield more or less elongated or bipolar structures. However, the same qualitative features as those seen in Figure 2 persist until the shocks run off our grid. Note that the nebulae in Figure 2 are evolved objects. Our simulations, on the other hand, are restricted to the first 1000 yr of evolution due to limited computational resources. This disparity can be partially reconciled by considering the scaling arguments presented in Icke et al. (1992b). We note also that our simulations demonstrate that the observationally important features develop quickly and persist throughout the evolution. Longer simulations, and those with stellar and fast wind evolution accounted for, are still required, however, before detailed comparisons with individual objects can be made.

One feature of the simulations meriting special note is a ringlike region of enhanced brightness where the lobes join the extremities of the barrel. As seen in Figure 2, these are likely to appear as two loops at the ends of the barrels, depending on inclination angle. They are regions where shocks associated with the barrel and the growing bipolar lobes intersect. Several nebulae exhibit these types of structures, most notably NGC 2610, its "twin" IC 289, the Saturn Nebula (NGC 7009), and perhaps most spectacularly, the Helix Nebula.

4. CONCLUSIONS

The numerical observations discussed in § 3 demonstrate that almost the entire range of PN morphologies can be embraced by the ISW model with radiation gasdynamics—a very reasonable, straightforward, observationally motivated physical model. The confrontation between simulations and observations is shown in Figure 2. We expressly do not insinuate that the model is an established paradigm. Rather, we spec-

ulate that the ISW approach to understanding the shapes and evolution of PNs is likely to be found in increasingly better accord with the gross observables of PNs as further numerical and observational work proceeds.

A declaration of success is premature. We have not yet explored the full range of extant observations of PN kinematic and ionization at high spatial resolution. (This facet of the work is progressing smoothly.) Also, the evolution of winds and UV radiation of the central nucleus has not been incorporated in the present models. To this end one of us is presently undertaking such computations (Mellema 1993) in order to better study the evolution of PN observables. Finally, variable grid sizes (to more accurately simulate shocks) and certain physical processes (e.g., conduction), are yet to be added to the computational model owing primarily to limited computation resources.

It is a pleasure to thank Alberto Noriega-Crespo for his continuing interest, advice, and suggestions about nebular hydrodynamics. B. B. and A. F. enjoyed partial support from grants made by the National Science Foundation (AST 89-13639) and the Netherlands Foundation for the Advancement of Pure Research (B78-302). All authors acknowledge the generous support for the international collaboration from NATO (grant 0898/87) and the Leids Kerkhoven-Bosscha Foundation as well as the hospitality of Sterrewacht Leiden and the University of Washington.

REFERENCES

Balick, B. 1987, AJ, 94, 671 (B87)
Balick, B., Gonzalez, G., Frank, A., & Jacoby, G. 1992, ApJ, 392, 582
Balick, B., Preston, H. L., & Icke, V. 1987, AJ, 94, 1641 (BPI87)
Balick, B., Rugers, M., Terzian, Y., & Chengalur, J. 1993, in preparation
Dalgarno, A., & McCray, R. 1972, ARA&A, 10, 375
Dyson, J. E., & Williams, D. A. 1980, Physics of the Interstellar Medium (Manchester: Manchester Univ. Press)
Frank, A. 1992, Ph.D. thesis, Univ. Washington
———. 1993, in preparation
Frank, A., & Mellema, G. 1993, in preparation
Icke, V. 1991, A&A, 251, 369
Icke, V., Balick, B., & Frank, A. 1992a, A&A, 253, 224 (IBF92)
Icke, V., Mellema, G., Balick, B., Eulderink, F., & Frank, A. 1992b, Nature, 355, 524
Icke, V., Preston, H. L., & Balick, B. 1989, AJ, 97, 462 (IPB89)
Kahn, F. D., & Breitschwerdt, D. 1990, MNRAS, 242, 505
Kahn, F., & West, K. A. 1985, MNRAS, 212, 837
Kwok, S., & Volk, K. 1985, A&A, 153, 79
Mellema, G. 1993, in preparation
Mellema, G., Eulderink, F., & Icke, V. 1991, A&A, 252, 718 (MEI91)
O'Dell, R., Weiner, L. D., & Chu, Y.-H. 1990, ApJ, 362, 226
Soker, N. 1989, ApJ, 340, 927
———. 1990, AJ, 99, 1869
Zhang, G., & Kwok, S. 1991, A&A, 250, 179

PLATE L2

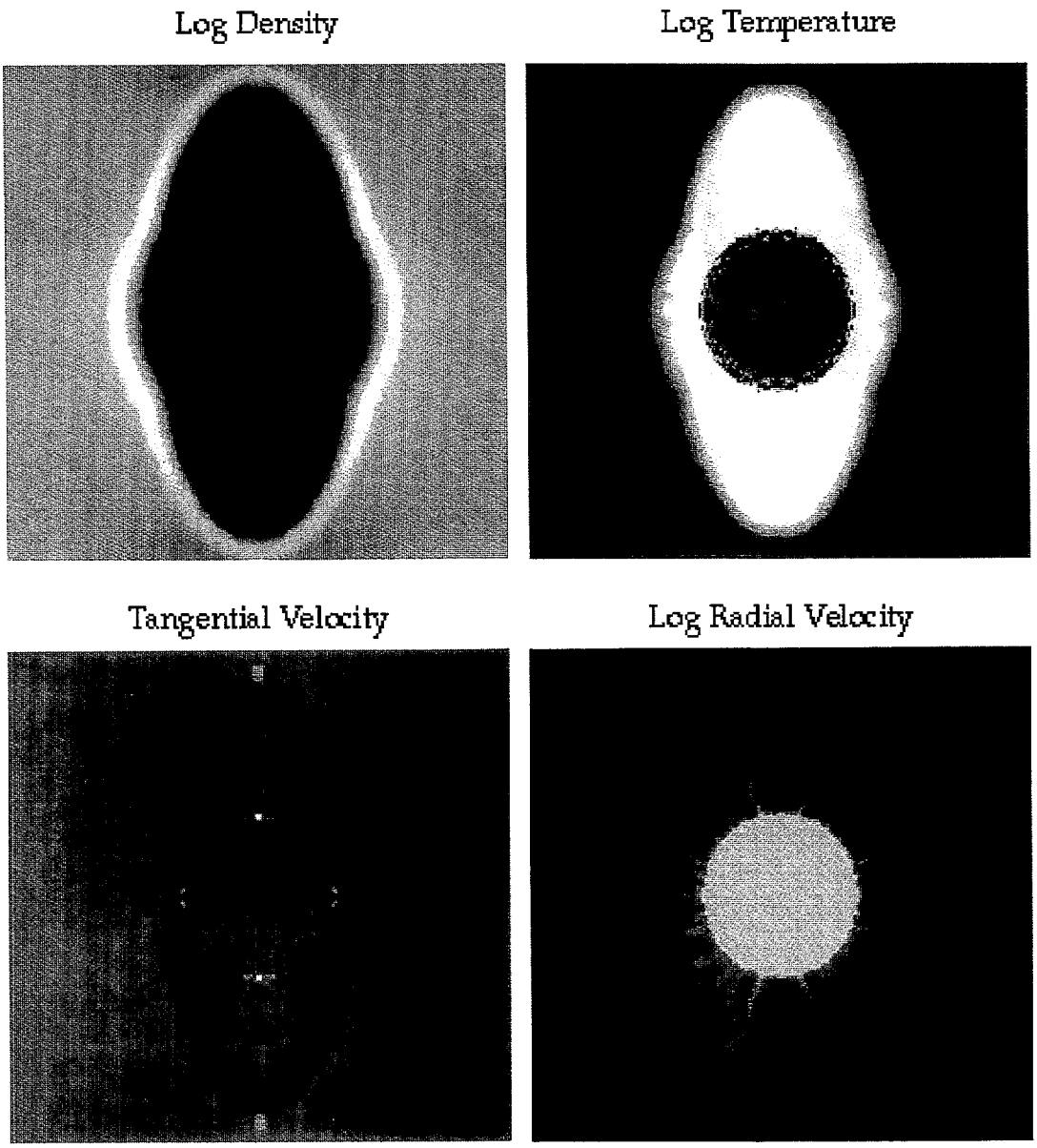

FIG. 1.—Mass density (log), temperature (log), radial velocity (log), and tangential velocity as a function of position after 900 years of evolution. The initial and boundary conditions are described in the text.

FRANK et al. (see 404, L26)

1993ApJ...404L..25F

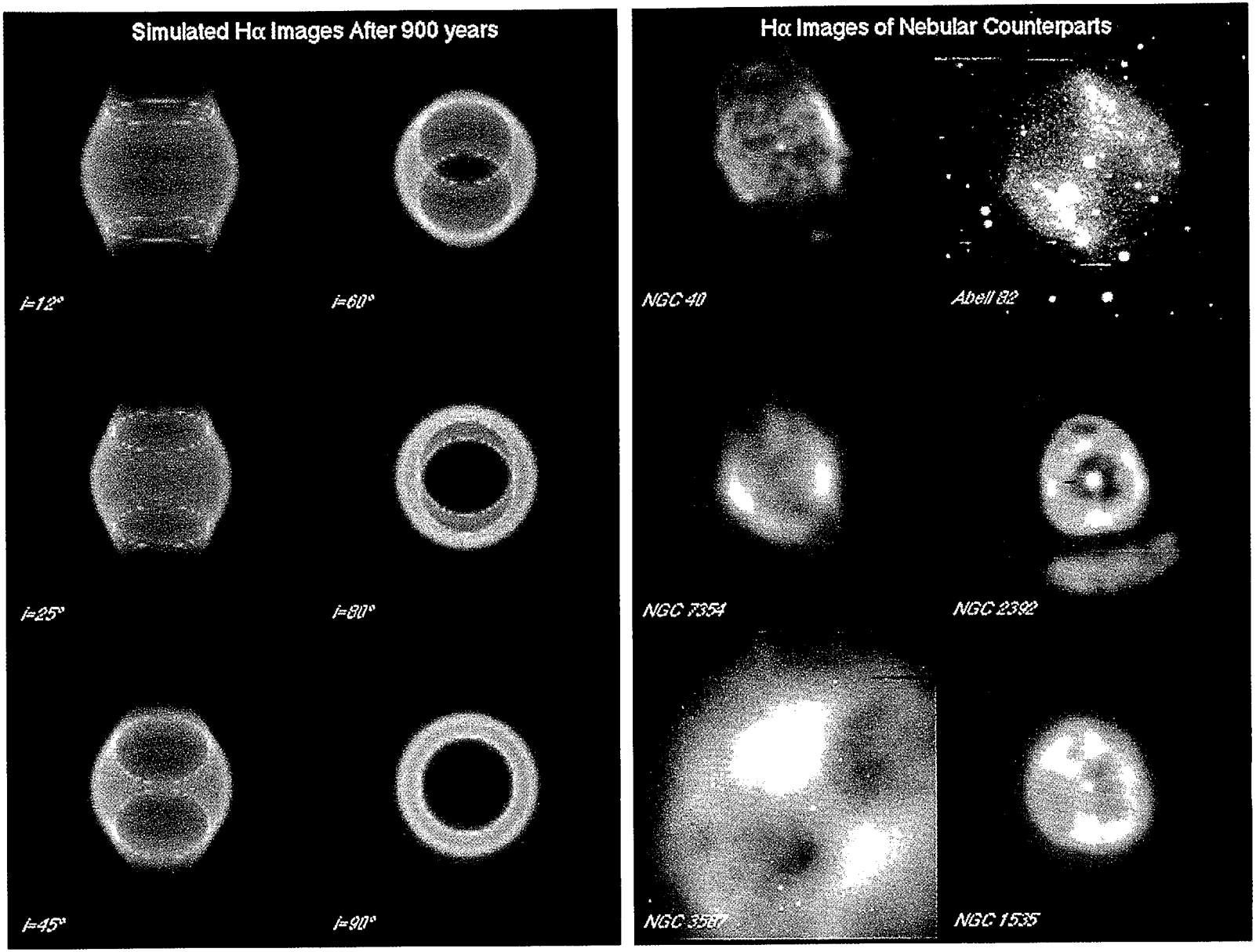

FIG. 2.—Synthesized, tilted, and projected intensity distribution in the light of Hα for the model of Fig. 1 after 900 yr. The panels represent the logarithm of the expected CCD image that would be obtained through a narrow filter for various nebular inclination angles *i*. Shown on the right are Hα images of likely nebular counterparts corresponding to each inclination in the left panel. An [N II] image is used for Abell 82 because the Hα image is so noisy. The images are taken from B87.